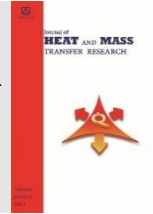




Semnan University



Multi Objective Optimization of Shell & Tube Heat Exchanger by Genetic, Particle Swarm and Jaya Optimization Algorithms: Assessment of Nanofluids as the Coolant

Ali Karimi Senejani^a, Zahra Baniamerian^{*,b}

^a Mechanical Energy and Engineering Department, Shahid Beheshti University, Tehran, Iran

^b Department of Mechanical Engineering, Tafresh University, Tafresh, Iran.

PAPER INFO

Paper history:

Received: 2021-07-13

Revised: 2022-01-02

Accepted: 2022-01-05

Keywords:

Multi objective;
Optimization;
Shell and tube heat exchanger;
Genetic algorithm;
Particle swarm;
Algorithm, Jaya;
Algorithm, Nanofluid.

ABSTRACT

In this study, the design of a nanofluid driven shell and tube heat exchanger is optimized, for the first time, by use of three multi objective algorithms. Two different operating conditions are investigated to compare the performance of the algorithms based on an economic model (cost function). Based on the obtained results, the Genetic, Particle Swarm and Jaya optimization algorithms can all improve the design. The amount of design improvement by each method is 9.66%, 10.63% and 10.9% respectively. Also from the view point of optimization time, Jaya optimization algorithm has relatively less CPU time than the other two algorithms, which in fact, reduces computational costs in complicated computations. Finally, due to the good performance of Jaya optimization algorithm in comparison with other considered algorithms, the performance of the heat exchangers is evaluated for using Ag, TiO₂ and Al₂O₃ nanofluids of 0.5% to 5 vol.% by this algorithm. A performance evaluation factor (PE) is introduced as the criterion for simultaneous investigation of thermal and hydraulic performance of nanofluids. The results show that silver nanofluid, among other ones has better performance.

DOI: 10.22075/jhmtr.2022.23959.1350

© 2022 Published by Semnan University Press. All rights reserved.

1. Introduction

The optimal solution, in other words, the optimization, is actually the best answer according to the limitations. Optimization can be defined as mathematical planning in economics and management refers to choosing the best member of a set of achievable members. In the simplest form, it is attempted to systematically select data from an accessible set and calculate the value of a real function and determine its maximum and minimum values. Based on the above definition, optimization can be applied in various applications. One of the widely used equipment in various industries is the heat exchanger which is applied to provide heat transfer between two or more fluids at different temperatures. Heat exchangers are widely used

in industries such as power plants, refineries, petrochemicals, nuclear, food industries, air conditioning, manufacturing processes, etc. Among the different types of heat exchangers, the shell & tube heat exchangers are widely used in industry, (Figure 1). This wide application can be justified by its versatility, strength, reliability and usability over a wide range of operating temperatures and pressures. On the other hand, due to the demand for higher capacity heat exchangers and at the same time lower weight and size and lower fuel consumption due to increased fuel costs, designers have been able to optimize heat exchangers for their intended purposes. In most cases, heat exchangers with the highest efficiency and lowest costs (including initial and operating costs) are desired. Since heat exchanger optimization is very important in

*Corresponding Author: Zahra Baniamerian
Email: amerian@tafreshu.ac.ir

terms of performance, finding a suitable method for optimization is very important. In most engineering issues including design of heat exchangers, many parameters are involved with nonlinear relationships. The combination of these relationships gives rise to more complex functions that the usual mathematical solving methods to optimize such functions are either very difficult or in some cases impossible.

Sadeghzadeh et al. [1] optimized a shell & tube heat exchanger by single objective algorithms of genetic and particle swarm although based on the obtained results, they found particle swarm better than genetic algorithm.

Rao et al. [2] introduced the Jaya multi-objective optimization algorithm and then examined its details. According to the results, this algorithm has a high convergence rate than other algorithms. They also examined various applications of this algorithm for example in the machining process.

Valipour et al. [3] first used the Big Bang multi-objective optimization algorithm. They also used the Bell-Delaware method to estimate the heat transfer coefficient. Finally, by considering the two objective functions of cost and efficiency and Comparison of the results with the multi-objective genetic optimization algorithm, they concluded that the results of the Big Bang algorithm are better and more effective than the genetic algorithm.

Sadeghzadeh et al. [4] considered a shell & tube heat exchanger with fin. They also used the Delaware method to estimate the heat transfer coefficient. They examined the objective functions with the multi-objective and single-objective genetic algorithms that merged the answers and compared the results of both approaches.

John et al. [5] investigated a matrix heat exchanger with multi-objective and single-objective genetic optimization algorithm for optimizing the surface of heat exchanger, which eventually obtained the promising results.

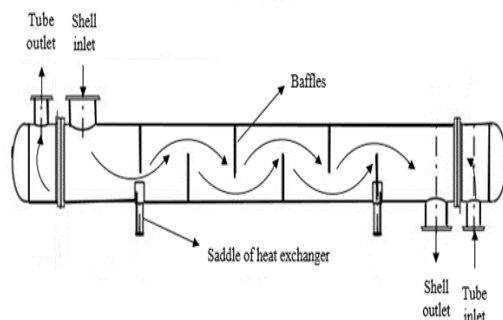


Figure 1. Schematic of shell and tube heat exchanger

Turgut [6] investigated the thermal design of a plate frame heat exchangers based on Global Best Algorithm. He employed some basic perturbation methods to achieve optimum solution and more focused on exploitation of the promising solutions rather than exploring of the unvisited paths of the search domain. He considered eight decision variables for the heat exchanger and applied them to sensitivity testing to examine the impact of each.

Taghilou et al. [7] investigated a double-pipe heat exchanger using Brent optimization algorithm and reported that in all conditions the generated entropy is reduced that leads to reduced pump power consumption and construction cost of heat exchanger.

Christian et al. [8] introduced and investigated the topology optimization model for heat transfer issues and especially heat exchangers and reported that this model is a suitable model for heat exchanger optimization based on the results.

Ghorbani et al. [9] used a genetic algorithm to optimize the heat exchanger. They reported a 15% increase in heat exchanger efficiency and a significant decrease in pressure drop as a result of optimization.

Hajabdollahi et al. [10] examines the effects of a tube fitted with twisted tape on the optimal design of a fin-and-tube heat exchanger. They optimized heat exchanger with pressure drop and effectiveness as objective functions and then found a marginal point for effectiveness and the margin value occurred at higher effectiveness.

Zhao et al. [11] considered the effect of heat transfer coefficient and pressure drop in order to investigate the parameters affecting the heat exchanger and finally presented a model which can be considered as a variable heat transfer coefficient which increases the accuracy of optimization.

Najafi et al. [12] optimized a multi-objective plate heat exchanger using genetic algorithm. They observed that an increase in pressure drop would increase pump costs operational costs in turn. On the other hand, any attempt to reduce the pressure drop will reduce the overall heat transfer which results in an increase in the heat transfer level. Therefore, finding a new generation of coolants with high potential capacities of heat transfer seems effective.

Shoheib et al. [13] investigated the effect of the tube material on thermal stress. Finally, based on the analyzed materials, copper had the lowest thermal stress and steel had the highest safety.

Balamurugan et al. [14] Investigated the effect of different parameters on the performance of the shell & tube heat exchanger.

In references [14-15] can be found more research on the optimization of heat exchangers.

Nanofluids are new class of dilute suspensions that consist of a base fluid with nanosized particles (1–100 nm) suspended within [19]. Applied nano particles can be commonly a metal or metal oxide that increase the overall thermal conductivity of the fluid. Water and ethylene glycol are the most common base fluids in preparation of nanofluids.

Nanofluids were first developed around 1995, with the specific aim of increasing thermal transport of conventional heat transfer fluids, which have now evolved into a promising nanotechnology-based thermo-fluids and energy area [19]. Nanofluids facilitate better heat transfer compared with a pure fluid due to their improved thermos-physical properties in the presence of nanoparticles. Also, because of the dynamic behavior of nanoparticles suspended in the base fluid along with the Brownian motions, the heat transfer coefficient of these fluids is higher than their base fluids [19]. Therefore, nanofluids can be a good choice to be applied as a coolant in many thermal objectives like heat exchangers and become a new generation of coolants which can be engineered in thermophysical properties. There are some researches in the literature devoted to investigation of nanofluids in heat exchangers.

Wael et al. [20] studied numerically the turbulent heat transfer and pressure drop of nanofluid in a coiled tube-in-tube heat exchanger. They reported that by increasing the volume concentration of nanofluid, the heat transfer coefficient increased, which in turn reduced the size of the heat exchanger.

Aliabadi [21] analyzed the heat transfer and flow characteristics of the sinusoidal-corrugated channel with Al_2O_3 -water nanofluid by a 2-D numerical simulation. One of the most important results presented by him is that the nanofluid offers the higher values of PEC (Performance Evaluation Criteria) compared to the base fluid, and the higher values of PEC are obtained for the nanofluids with the larger volume concentration of Al_2O_3 nanoparticles.

There are few optimization studies, in the literature, for heat exchangers with nanofluids which mostly assess thermal performance. Although due to applying different algorithms for optimization, different results are obtained. In the present study the thermal and hydraulic performances of a shell and tube heat exchanger for two different operating conditions are optimized by three popular multi-objective genetic, particle swarm and jaya optimization algorithms. The most effective algorithm is then

applied to optimize the performance of the heat exchanger for various nanofluids based on the introduced PEC factor. The PEC factor, in fact, can evaluate thermal and hydraulic performance of the heat exchanger simultaneously. The novelty of the purpose is optimized designing a nanofluid driven shell and tube heat exchanger with three different optimization algorithms (Genetic, Particle Swarm and Jaya optimization algorithms) and Comparison of the performance of each algorithm in design improvement. These algorithms have not been ever investigated for nanofluid performance to integrate hydro-thermal behavior together with the design optimization.

2. Optimization algorithms

Optimization algorithms are divided into two categories of exact and approximate algorithms. Exact algorithms are able to find the optimal solution accurately but are not efficient in the case of complicated optimization problems and their execution time increases exponentially with the dimensions of the issues. Approximation algorithms are able to find good (near optimal) solutions in short time for difficult optimization problems. The approximate algorithms are also divided into three categories: heuristic and meta-heuristic and hyper-heuristic. In computer science, artificial intelligence and mathematical optimization, a technical heuristic algorithm is designed to solve a problem more quickly or to find an approximate solution when classical methods are too slow or fail to find the exact solution.

2.1. Genetic algorithm

The genetic algorithm, proposed based on Darwin's theory, is a widely used optimization method. This theory states that inferior creatures pass away while superior creatures remain. In this optimization algorithms search procedure are inspired by natural selection. Collections of design variables are codified by fixed/variable-length sequences, just similar to chromosomes or individuals in biologic systems. Similar to what is naturally seen, each chromosome contains several design variables, known as genes and shows one solution point in the search space. Hereditary algorithms are repetitive processes with several repetition stages called generation. The corresponding set of solutions is called population. The algorithm begins with seeding, and in this regard, the first population is randomly/selectively selected among possibilities in the search space. Directive searching toward optimum points in the genetic

algorithm is based on statistical methods. In the process of natural selection, the fitness of this generation for the next generation is the basis of population selection. The new population, which is usually more fit, replaces the previous one and the cycle continues. The search is deemed completed as it achieves the maximum intended generation or a convergent result is obtained or the stop criterion is met. The flowchart of the GA is given in Figure 2.

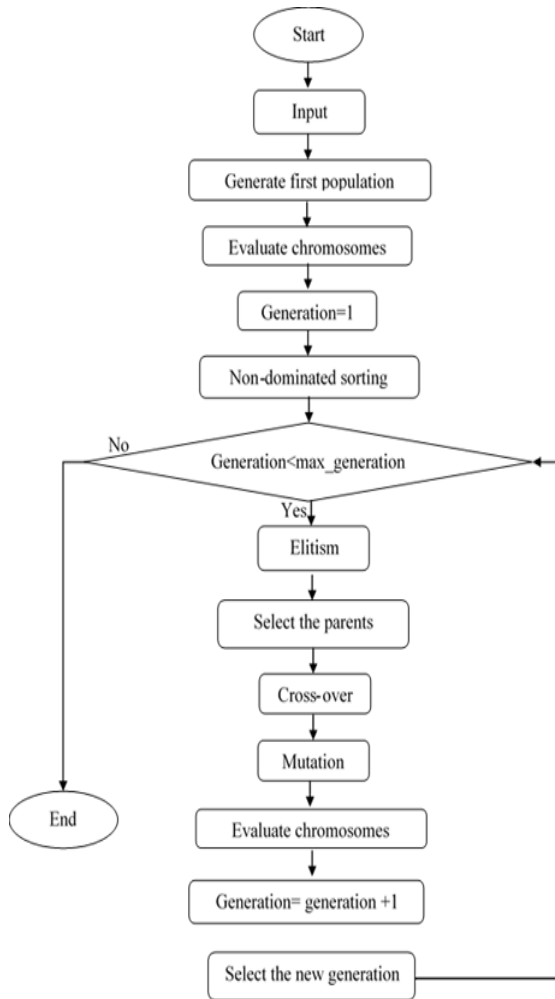


Figure 2. Flowchart of MOGA. [22]

2.2. Particle swarm algorithm

First introduced by Eberhat and Kennedy in 1995, the particle swarm optimization (PSO) algorithm imitates the way fish and birds swarm search for food. Each particle is in fact a solution to a problem. PSO distincts from other optimization methods (like GA) due to performance simplicity and higher velocity. Particles in PSO are responsible to find a global optimum point in a search space. This mimics how birds (particles) use whole set information to determine their orientation. Accordingly, the collective location of the swarm and the best

individual location of particles per time are calculated, and the new search orientation consists of the two orientations and the previous one [1].

In a search space of D dimension, if the best individual location of a particle is shown by $\vec{P}_1 = c_1(\vec{P}_{11}, \vec{P}_{12}, \dots, \vec{P}_{1D})$ and the best location of the overall particle by $\vec{g} = c_1(g_1, g_2, \dots, g_D)$, The best location in the vicinity of each particle is introduced by $\vec{n}_1 = c_1(\vec{n}_{11}, \vec{n}_{12}, \dots, \vec{n}_{1D})$. Displacement of particles after determination their velocity is then can be calculated by [1]:

$$\vec{x}(t) = \vec{x}(t-1) + \vec{v}(t) \quad (1)$$

Where

$$\vec{v}(t) = \vec{v}(t-1) + \vec{F}(t-1) \quad (2)$$

The force applied to the particle is simulated by the best individual particle location and the best particle collective location as two springs attached to the particle. The first spring is driven to the best individual experience and the second one to the best swarm experience [1]:

$$\vec{F}_{i-1} = c_1(\vec{P}_{i-1} - \vec{x}_{i-1}) + c_2(\vec{g}_{i-1} - \vec{x}_{i-1}) \quad (3)$$

Here, c_1 and c_2 accounts for Hook spring coefficients or acceleration coefficients that are usually set on value 2. The particle velocity is finally calculated at dimension d and the next repetition is as follows [1]:

$$v_{id}(t) = \omega v_{id}(t-1) + c_1 rand_1 (\vec{P}_{i-1}(t-1) - \vec{x}_{i-1}(t-1)) + c_2 rand_2 (\vec{n}_{i-1}(t-1) - \vec{x}_{i-1}(t-1)) \quad (4)$$

Random numbers $rand_1$ and $rand_2$ are in the range 0 - 1. The term ω accelerates convergence at the local optimum, although it is not as useful for very high values.[1] A PSO flow chart is demonstrated in Figure 3.

2.3. Multi objective Jaya algorithm

In the Jaya algorithm P the upper and lower bounds of the process variables are employed to generate initial solution randomly. Thereafter, variables of each solution is stochastically updated using Eq. (5). Here f is the objective function with 'd' number of design variables. The objective function value, corresponding to the best solution is shown by f_{best} and that corresponding to the worst solution is shown by f_{worst} [2].

$$A(i+1, j, k) = A(i, j, k) + r(i, j, 1)(A(i, j, b) - |A(i, j, k)|) - r(i, j, 2)(A(i, j, w) - |A(i, j, k)|) \quad (5)$$

Where b and w accounts for the index of the best and worst solutions among the population. i,j,k are the index of iteration, variable, and candidate solution. $A(i,j,k)$ means the j th variable of k th candidate solution in i th iteration. $r(i,j,1)$ and $r(i,j,2)$ are numbers generated randomly in the range of $[0,1]$. The random numbers $r(i,j,1)$ and $r(i,j,2)$ act as scaling factors and have good diversity. The principle objective of the Jaya algorithm is to improve the fitness of each candidate solution in the population. Therefore, the Jaya algorithm, in principle, by updating the values of the variables, forces the magnitude of the objective function of each solution towards the best solution. The updated (new) solutions are then compared with the corresponding old solutions and only the solutions with better objective function value are considered for the next generation.[2]

Multi-objective Jaya Optimization algorithm is a multi-objective version of the single- objective Jaya optimization algorithm that is used to investigate multi-objective topics. The main equation of updating solutions in the multi-objective Jaya algorithm based on Eq. (5) is such as single-objective version. In the multi-objective version of this algorithm, non-dominated sorting and crowding distance calculation mechanisms is used. The crowding-distance (CD) operator is an introduced operator which is used for calculation density of solutions in the search space. this operator has been used in different multi-objective optimization algorithms. In single-objective optimization it is easy to select the best solution and obtain the optimal solution based on the objective function value. But in multi-objective optimization it is difficult to choose the worst and best solution from the collection of solutions based on answers. In the MO¹-Jaya algorithm, the role of finding and choosing the best and worst solutions is done by Comparison of the rank assigned to the solutions based on the non-dominance concept and the crowding distance value. At first a population is randomly generated with NP² number of solutions and then this initial population is sorted and ranked based on the non-dominance concept. The solution with the highest rank (rank=1) is chosen as the best solution and the solution with the lowest rank is chosen as the worst solution. In case, when there are several solutions with the same rank, the solution is chosen as the best solution with the highest crowding distance and vice versa. This method is actually to ensure the choice of best solution in the search space. After choosing the

best and the worst solution, the solutions are updated by using Eq. (1). After updating the solutions, the set of updated solutions (new solutions) is added to initial population and make a set of 2NP solutions. These new solutions are again sorted and ranked based on the non-dominance concept and the crowding distance value for each solution is computed. Now based on new ranking and crowding-distance, good solutions are chosen [2]. Figure 4 shows the flowchart of MO-Jaya.

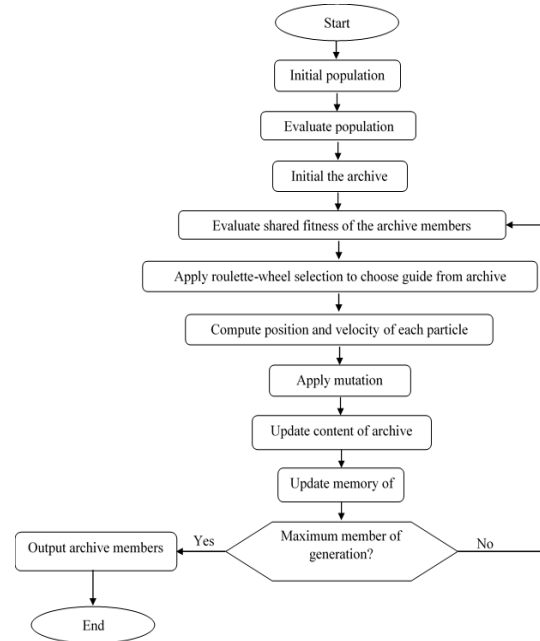


Figure 3. Flowchart of MOPSO [23].

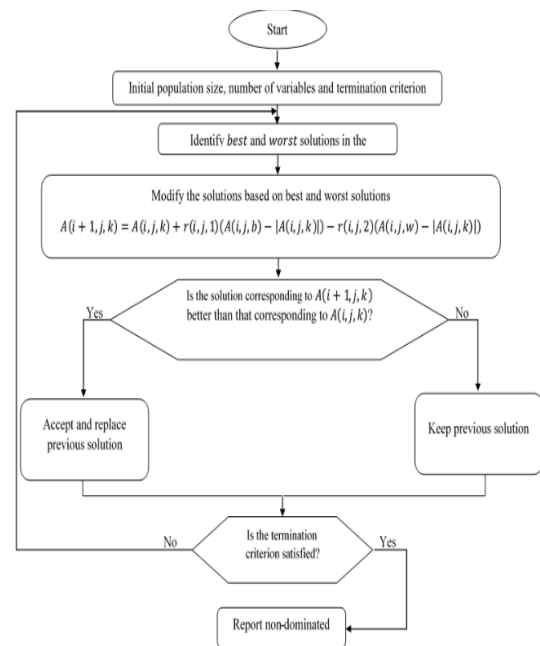


Figure 4. Flowchart of MO-Jaya [2].

¹ Multi objective

² Number of solution

Each of these algorithms has advantages and disadvantages. For example, in the genetic algorithm, due to the competition of answers and the selection of the best from the population, I will most likely reach the global optimal point. It is also easy to implement, but the most important problem of this algorithm is its high computational cost. Of course, compared to some algorithms, the genetic algorithm does not have much computational cost due to its metaheuristic nature. Also the particle swarm algorithm has advantages such as high convergence speed, better flexibility against local optimal problem, cooperation and information sharing between particles and ease of implementation and execution, and in contrast has disadvantages such as early convergence, local optimization and Decreasing population diversity.

The Jaya algorithm is also one of the most innovative algorithms used for many problems that has a high speed of convergence. Genetic algorithms and particle swarm already have been used to optimize heat exchangers, and we intend to use the genetic algorithm, particle swarm, and Jaya in heat exchanger and ultimately nanofluid optimization for comparison.

For comparing this algorithms, we used a economic model for estimating the total cost of heat exchanger. This economic model includes operating costs and investment costs. Actually to compare algorithms with each other, we optimize the cost function as important parameter for deciding to reduce it by coding the cost function in MATLAB software.

3. Mathematical modeling

3.1. Shell & tube heat exchanger

The following equation is used to calculate the heat transfer area (A) of heat exchanger [24]:

$$A = \frac{Q}{UF\Delta T_{lm}} \quad (6)$$

In Eq. (6) U_o is the overall heat transfer coefficient of heat exchanger, ΔT_{lm} is the log-mean temperature difference and F is correction factor for the number of tube passes.

The outer overall heat transfer coefficient (Neglecting the thermal resistance of the wall) is calculated as follows [22]:

$$U_o = \left[\frac{1}{h_o} + R_{f,o} + \frac{d_o}{d_i} \left(R_{i,f} + \frac{1}{h_i} \right) \right]^{-1} \quad (7)$$

$$d_i = 0.8d_o \quad (8)$$

where d_i , d_o , $R_{i,f}$, $R_{o,f}$, h_i and h_o are inside and outside tube diameters (m), tube- and shell-side fouling resistances ($m^2 \cdot K/W$), and tube and shell-

side heat transfer coefficients ($\frac{W}{m^2 \cdot K}$), respectively.

Based on LMTD (logarithmic average of the temperature difference) method the log-mean temperature difference for a shell and tube heat exchanger can be calculated as follows [2]:

$$\Delta T_{lm} = \frac{(T_{h1} - t_{c2}) - (T_{h2} - t_{c1})}{Ln \frac{T_{h1} - t_{c2}}{T_{h2} - t_{c1}}} \quad (9)$$

The correction factor F is defined as follows [20]:

Where

$$F = \frac{(\sqrt{1+R^2} Ln \left(\frac{1-P}{1-RP} \right))}{(R-1) Ln \left(\frac{2-P((R+1)-\sqrt{1+R^2})}{2-P((R+1)+\sqrt{1+R^2})} \right)} \quad (10)$$

Where

$$R = \frac{T_{h1} - T_{h2}}{t_{c2} - t_{c1}} \quad (11)$$

$$P = \frac{t_{c2} - t_{c1}}{T_{h1} - T_{h2}} \quad (12)$$

3.1.1. Tube side

The tube-side heat transfer coefficient h_i ($\frac{W}{m^2 \cdot K}$), based on Delaware method can be determined as follows [25-27]:

$$\text{if } \left(\frac{Re_t * Pr_t}{L} \right)^{\frac{1}{3}} \left(\frac{\mu}{\mu_w} \right)^{0.14} > 2$$

$$h_i = \left(\frac{k_t}{d_i} \right) 0.027 (Re_t^{0.8}) Pr_t^{0.4} \left(\frac{\mu}{\mu_w} \right)^{0.14} \quad (13)$$

for $Re_t > 10^4$

$$h_i = \left(\frac{k_t}{d_i} \right) 1.86 \left(\frac{Re_t d_i Pr_t}{L} \right)^{\frac{1}{3}} \left(\frac{\mu}{\mu_w} \right)^{0.14} \quad (14)$$

for $Re_t < 2100$

$$\text{Otherwise if } \left(\frac{Re_t * Pr_t}{L} \right)^{\frac{1}{3}} \left(\frac{\mu}{\mu_w} \right)^{0.14} < 2$$

$$h_i = 3.66 \frac{k_t}{d_i} \quad (15)$$

Here, k_t , Pr_t , μ and μ_w are the thermal conduction coefficient of fluid inside the tube ($W/m \cdot K$), the tube-side Prandtl number, the viscosity and fluid viscosity (Pa.s) evaluated at the average temperature of the tube wall.

Also, the tube side Reynolds number Re_t is calculated as follows [25]:

$$Re_t = \frac{\dot{m}_t d_i}{\mu_t A_{ot}} \quad (16)$$

In Eq. (16) \dot{m}_t is the tube side mass flow rate (kg/s) and A_{ot} is tube-side flow cross sectional area (m^2) per tube pass, expressible as [27]:

$$A_{ot} = \frac{\pi d_i^2 N_t}{4n_p} \tag{17}$$

The number of heat exchanger tubes is estimated by [28] :

$$N_t = k_1 \left(\frac{D_{totl}}{d_o}\right)^{n_1} \tag{18}$$

Also, D_{otl} is the tube bundle outer diameter and the coefficient values K_1 and n_1 are determined based on the flow arrangement and number of passes from Table 1. [29]:

Table 1. Values of coefficients K_1 and n_1 for $Pt = 1.25$ do [1].

| Number of passes | Triangular pitch | | Square and rotated square | |
|------------------|------------------|-------|---------------------------|-------|
| | K_1 | n_1 | K_1 | n_1 |
| 1 | 0.319 | 2.142 | 0.215 | 2.207 |
| 2 | 0.249 | 2.207 | 0.156 | 2.291 |
| 3 | 0.175 | 2.285 | 0.158 | 2.263 |

The inside tube pressure drop Δp_t (Pa) base on Delaware method can be calculated as follows [26]:

$$\Delta p_t = \frac{\vartheta_t}{2} \left(\frac{f_t L}{d_i} + y\right) n_p \tag{19}$$

here, y is a constant value, Numerous values have been reported, y can be 4 or 2.5. Also, f_t is the drag friction factor for turbulent flow, which can be calculated by following equation [29]:

$$f_t = 0.046(Re_t)^{-0.25} \tag{20}$$

3.1.2. Shell side

Also, for calculating the shell-side heat transfer coefficient Delaware method suggested following equations [30]:

$$h_o = h_{id} j_c j_b j_s j_r \tag{21}$$

$$h_{id} = j_{id} C_p \left(\frac{\dot{m}_s}{A_{o,cr}}\right) \left(\frac{k_s}{C_p \mu_s}\right)^{\frac{2}{3}} \left(\frac{\mu_s}{\mu_{s,w}}\right)^{0.14} \tag{22}$$

$$j_{id} = a_1 \left(\frac{1.33}{\frac{p_t}{d_o}}\right)^a (Re_s)^{a_2} \tag{23}$$

$$b = \frac{a_3}{1 + (0.14 Re_s^{a_4})} \tag{24}$$

$$\frac{p_t}{d_o} = 1.25 \tag{25}$$

$$A_{o,cr} = L_{b,c} [d_s - D_{otl} + 2 \frac{D_{ctl}}{x_l} (p_t - d_o)] \tag{26}$$

$$D_{ctl} = D_{otl} - d_o \tag{27}$$

with a good approximation $j_c j_b j_s j_r = 0.6$.

To determine the shell-side pressure drop the Delaware method is used [29]:

$$\Delta p_s = [(N_b - 1) \Delta p_{b,id} R_b + N_b \Delta p_{w,id}] R_l + 2 \Delta p_{b,id} \left(1 + \frac{N_{r,cw}}{N_{r,cc}}\right) R_b R_s \tag{28}$$

here, $N_{r,cw}$ is the number of effective tube rows crossed during flow through one window zone in a segmentally baffled shell-and-tube heat exchanger, $N_{r,cc}$ is the number of effective tube rows crossed during flow through one cross flow section and $\Delta p_{b,id}$ is the pressure drop for liquid flow in an ideal cross flow between two baffles, and is expressible as follows [29]:

$$\Delta p_{b,id} = 4 f_{id} \frac{G_s^2}{2 \rho_s} \left(\frac{\mu_{s,w}}{\mu_s}\right)^{0.14} N_{r,cc} \tag{29}$$

In Eq. (29), f_{id} is the friction factor for flow through an ideal tube bank, which can be determined as follows [29]:

$$f_{id} = b_1 \left(\frac{1.33}{\frac{p_t}{d_o}}\right)^b (Re_s)^{b_2} \tag{30}$$

and

$$b = \frac{b_3}{1 + (0.14 Re_s^{b_4})} \tag{31}$$

Values for coefficient b_1 , b_2 , b_3 and b_4 are showed in Table 2. The pressure drop associated with an ideal window section ($\Delta p_{w,id}$) is obtained by [29]:

$$\Delta p_{w,id} = (2 + 0.6 N_{r,cw}) \frac{G_s^2}{2 \rho_s} \tag{32}$$

Also R_b is between 0.5 to 0.8 and R_l is between 0.4 to 0.5.

3.2. Cost function

In this investigation, in order to compare the algorithms, we use the total cost as the main objective function. The total cost includes the investment cost and the operating cost with taking the pumping cost in to consideration [30]:

$$C = C_{in} + C_{op} \tag{33}$$

The operating cost C_{op} (€) and the investment C_{in} (€) for the shell and tube heat exchanger with stainless steel tube can be determined respectively as follows [31]:

$$C_{in} = 8000 + 59.2A^{0.91} \tag{34}$$

$$C_{op} = \sum_{k=1}^{n_y} \frac{C_o}{(1 + \lambda)^k} \tag{35}$$

Table 2. Colburn factor Jid coefficients and ideal friction factor fid [29].

| Layout angle(°) | Reynolds number | a ₁ | a ₂ | a ₃ | a ₄ | b ₁ | b ₂ | b ₃ | b ₄ |
|-----------------|-----------------------------------|----------------|----------------|----------------|----------------|----------------|----------------|----------------|----------------|
| 30 | 10 ⁵ – 10 ⁴ | 0.321 | -0.388 | 1.450 | 0.519 | 0.372 | -0.123 | 7.00 | 0.500 |
| | 10 ⁴ – 10 ³ | 0.321 | -0.388 | - | - | 0.486 | -0.152 | - | - |
| | 10 ³ – 10 ² | 0.593 | -0.477 | - | - | 4.57 | -0.476 | - | - |
| | 10 ² – 10 | 1.360 | -0.657 | - | - | 45.100 | -0.973 | - | - |
| | <10 | 1.400 | -0.667 | - | - | 48.000 | -1.00 | - | - |
| 45 | 10 ⁵ – 10 ⁴ | 0.370 | -0.369 | 1.930 | 0.500 | 0.303 | -0.126 | 6.59 | 0.520 |
| | 10 ⁴ – 10 ³ | 0.370 | -0.369 | - | - | 0.333 | -0.136 | - | - |
| | 10 ³ – 10 ² | 0.730 | -0.500 | - | - | 3.500 | -0.476 | - | - |
| | 10 ² – 10 | 0.498 | -0.656 | - | - | 26.200 | -0.913 | - | - |
| | <10 | 1.550 | -0.667 | - | - | 32.00 | -1.000 | - | - |
| 90 | 10 ⁵ – 10 ⁴ | 0.370 | -0.395 | 1.187 | 0.370 | 0.391 | -0.148 | 6.30 | 0.378 |
| | 10 ⁴ – 10 ³ | 0.107 | -0.266 | - | - | 0.0815 | -0.022 | - | - |
| | 10 ³ – 10 ² | 0.408 | -0.460 | - | - | 6.0900 | -0.602 | - | - |
| | 10 ² – 10 | 0.9 | -0.631 | - | - | 32.1000 | -0.963 | - | - |
| | <10 | 0.97 | -0.667 | - | - | 35.000 | -1.000 | - | - |

Such that, C_o is the annual operational cost(€/year), n_y is the equipment life (year), and k is the annual inflation rate. The total operating cost is dependent on the pumping power, which overcomes the pressure drop for both the shell and tube side flows [31]:

$$C_o = p \cdot k_{el} \cdot \tau \quad (36)$$

$$p = \left(\frac{\dot{m}_t \Delta p_t}{\rho_t} + \frac{\dot{m}_s \Delta p_s}{\rho_s} \right) \frac{1}{\eta} \quad (37)$$

In Eq. (37), k_{el} is the unit price of electrical energy (€/kW h), P is the pumping power (W), τ is the hours of operation per year and η is the pump efficiency (-).

3.3. Nanofluids

Due to the presence of nanoparticles in the base fluid, some thermo-physical properties of the fluid become subject to change [32]. There have been several equations proposed for modeling and calculation of the thermophysical properties of nanofluids. In the present simulation, the density of nanofluid (ρ_{nf}) is obtained from the following equation [33]:

$$\rho_{nf} = \phi \rho_{np} + (1 - \phi) \rho_{bf} \quad (38)$$

where ρ_{bf} and ρ_{nf} are the mass densities of the based fluid and the solid nanoparticles, respectively.

The specific heat of nanofluid is also calculated from the following equation [33]:

$$C_{p,nf} = \phi C_{p,np} + (1 - \phi) C_{p,bf} \quad (39)$$

where $C_{p,bf}$ and $C_{p,np}$ are the specific heat of the based fluid and the solid nanoparticles, respectively.

To determine the conduction coefficient of the nanofluid, the equation of Zhao [32] is employed. In this model, in addition to Brownian motion, effects of nanoparticle clustering on volume fraction and conductivity is comprehensively considered. The other strength of this model is considering effects of formed nanolayer around the nanoparticles and Kapitza resistance on the nanofluid conductivity. Equation (40) expresses the final form of the Zhao model for conductivity [32].

$$k_{eff} =$$

$$\frac{k_{pe}(1 + 2\chi) + 2k_f + 2[k_{pe}(1 - \chi) - k_f]\phi_{fr}}{k_{pe}(1 + 2\chi) + 2k_f - [k_{pe}(1 - \chi) - k_f]\phi_{fr}} k_f + k_{Brownian} \quad (40)$$

where k_{pe} , χ , ϕ_{fr} , and $k_{Brownian}$ respectively accounts for thermal conduction due to nanolayer formation, nondimensional interfacial thermal resistance, modified particle volume fraction due to nanoparticles agglomeration, and the additional thermal conductivity due to the Brownian motion, which are calculated by Eqs. 40a to 40e.

$$k_{pe} = \frac{[(1 + \beta)^3(1 + 2\gamma) + 2(1 - \gamma)]\gamma}{(1 + \beta)^3(1 + 2\gamma) - (1 - \gamma)} k_p \quad (40a)$$

$$\chi = 2R_k k_l / d_p \quad (40b)$$

$$\phi_{fr} = \phi(1 + \beta)^3 \left(\frac{d_{fr}}{d_p} \right)^{3-D_{fr}} \quad (40c)$$

$$k_{Brownian} = A_0 \frac{d_f}{d_p} k_f Re_p^{A_1} Pr^{0.3333} \phi_{fr} \quad (40d)$$

where Re_p is the nanoparticle Reynolds number and defined as:

$$Re_p = \frac{\rho_{nf}}{\mu_{nf}} \sqrt{\frac{18k_B T}{\pi \rho_p d_p}} \quad (40e)$$

When nanoparticles are added to the fluid, along with the proved increase in heat transfer, the flow pressure drop increases too. As much as the first effect is desirable to improve the heat exchanger efficiency, the second effect is undesirable. In this regard to have a good evaluation on effects of nanofluids on overall performance of the considered heat exchanger a factor of performance evaluation criteria (PEC) is introduced to assess both effects simultaneously. The PEC is defined as [20]:

$$PEC = \frac{Nu_{n,f}}{Nu_w} \left(\frac{f_{n,f}}{f_w} \right)^{1/3} \quad (41)$$

Where:

$$f = \frac{2\Delta p d_h}{\rho v^2 L} \quad (42)$$

The correlation of Maiga et al. [34] is applied for calculation of the Nusselt number.

$$Nu_{n,f} = 0.085 Re_{nf}^{0.71} Pr_{nf}^{0.35} \quad (43)$$

4. Modeling

In this research, due to involving various interdependent parameters on the performance of the heat exchanger, three different multi-objective algorithms with two different operation conditions are applied to optimize the heat

exchanger design by coding the objective functions and correlations in MATLAB 2014R. At this step the working fluid of the heat exchanger is supposed to be pure and the performance of three different multi-objective optimization algorithms of Genetic, Particle Swarm and Jaya are compared together. The optimized heat exchanger, obtained from this stage, is then considered with various nanofluids as its working fluid and another optimization procedure is performed to find the best nanofluid (and vol. concentration) which lead to the optimum thermal and hydraulic performance.

The latter optimization is accomplished by the algorithm which showed the best performance in the first step. Silver, Titanium dioxide and Aluminum oxide water-based nanofluids of 0.5-5 vol.% are considered as the tube-side working fluid. The main criterion for evaluation of thermal and hydraulic performance is the PEC factor.

The first case study involves a heat exchanger which is supposed to be transferred between methanol and sea water, two tube-side passes, single shell-side pass and a triangular pitch layout [1]. The second case study involves a heat exchanger between two fluids (distilled water and raw water) with two tube-side passes, a triangular pitch arrangement and single shell-side pass. The specifications of these two case studies are demonstrated in Table 3.

Three objective functions are the overall heat transfer coefficient, the shell side pressure drop and the total cost. The selected decision variables include tube diameter, central baffles spacing and shell diameter. Lower and higher bounds for optimization decision variables for a given objective are given in Table 4. In both cases, the equipment life is taken to $n_y = 10$ (year); the inflation rate $k = 10\%$; the unit price of electricity $k_{el} = 0.12$ (€/kW h) and the working hours $\tau = 7000$ (h/year). Also, the baffle cut is taken to be 25% here.

Table 3. Inlet and outlet conditions and physical properties of fluids on the inside shell and tube [1].

| | Mass flow (kg/s) | Inlet temp (°C) | Outlet temp (°C) | Density (kg/s) | Specific heat (J/kg. K) | Viscosity (Pa. s) | Thermal conductivity (W/m. K) | Fouling resistance (W/m ² . K) |
|-----------------------------|------------------|-----------------|------------------|----------------|-------------------------|-------------------|-------------------------------|---|
| Case 1 | | | | | | | | |
| Shell side: methanol | 27.8 | 95 | 40 | 750 | 2840 | 0.00034 | 0.19 | 0.00033 |
| Tube side: sea water | 68.9 | 25 | 40 | 995 | 4200 | 0.00080 | 0.59 | 0.00020 |
| Case2 | | | | | | | | |
| Shell side: distilled water | 22.07 | 33.9 | 29.4 | 995 | 4180 | 0.00008 | 0.62 | 0.00017 |
| Tube side: raw water | 35.31 | 23.9 | 26.7 | 999 | 4180 | 0.00092 | 0.62 | 0.00017 |

Table 4. Lower bound and upper bound for design parameters [1].

| Parameter | Lower value | Upper value |
|----------------------------|-------------|-------------|
| Tubes outside diameter (m) | 0.01 | 0.051 |
| Shell diameter (m) | 0.1 | 1.5 |
| Central baffle spacing (m) | 0.05 | 0.5 |

Also the thermos-physical properties of Ag, TiO_2 and Al_2O_3 nanoparticles are also shown in Table 5.

Table 5. Thermo-physical properties of Ag, TiO_2 and Al_2O_3 nanoparticles [35].

| Nanoparticle | ρ_{np} (kg/m ³) | $C_{p,np}$ (J/kg. K) | k_{np} (W/m. K) |
|--|----------------------------------|----------------------|-------------------|
| Ag (Silver) | 10490 | 238.64 | 429 |
| TiO ₂ (Titanium dioxide) | 4230 | 690 | 8.3 |
| Al ₂ O ₃ (Aluminium dioxide) | 3950 | 785 | 30 |

5. Validation

In order to ensure the accuracy of the objective functions in codes, The obtained results based on Table 3 without optimizing are firstly compared with those reported in [1,33] that shown in Table 6 are set similar accordingly. The total cost function as the main function and the final result, According to the reported total cost which is 64480 (euro) and calculated total cost which is 62276 (euro) that has an error of approximately 3.5%. That is an acceptable deviation and can be seen in Table 6.

Table 6. Comparison between values in reference [1,36] and simulation results.

| Parameter | Refrence [1,36] | Present results | Mean verage erro(%) |
|------------------------------|-----------------|-----------------|---------------------|
| d_s (m) | 0.894 | 0.894 | 0 |
| L(m) | 4.83 | 3.98 | 17 |
| d_o (m) | 0.02 | 0.02 | 0 |
| P_t (m) | 0.025 | 0.025 | 0 |
| N_t (m) | 918 | 934(467-2Pass) | 2.7 |
| L_{bc} (m) | 0.356 | 0.356 | 0 |
| pr_t | 5.7 | 5.69 | 0.17 |
| Re_t | 14925 | 14932 | 0.046 |
| hi (W/m ² . K) | 3812 | 3534 | 7.29 |
| Δp_t (pa) | 6251 | 6479 | 3.64 |
| Δp_s (pa) | 35789 | 32070 | 10.39 |
| pr_s | 5.1 | 5.0821 | 0.35 |
| Re_s | 18381 | 18292 | 0.48 |
| ho (W/m ² . K) | 1573 | 2033 | 29.24 |
| U_o (W/m ² . K) | 738 | 710 | 3.79 |
| A(m ²) | 230 | 237 | 3.043 |
| C_{tot} (Euro) | 64480 | 62276 | 3.41 |

6. Results and discussion

As mentioned earlier, we optimized the three objective functions by three decision variables for a heat exchanger with two different conditions.

For the first case study, the optimization results for the multi-objective Genetic, Particle Swarm and Jaya optimization algorithms can be seen in Figures 5 and 6. According to Figure 5, the results do not differ much from one another.

It can also be found from the figure that as the heat transfer coefficient increases, the costs decrease. Surface elevation also has a range that is determined by the constraints. In other words, not all the points specified in the optimization graphs can be used.

It can also be observed from Figure 6 that the optimization results of the Particle Swarm at a constant pressure drop showed better results than the Genetic algorithm. And the jaya algorithm results seems better than the Particle Swarm. It can also be seen that the optimization in the approximate range of 10 (kPa) to 40 (kPa) is economical due to the increasing cost.

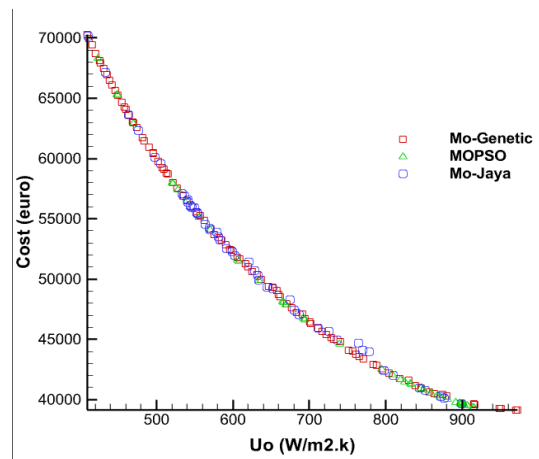


Figure 5. Comparison chart of three algorithms in terms of cost-overall heat transfer coefficient for case study 1.

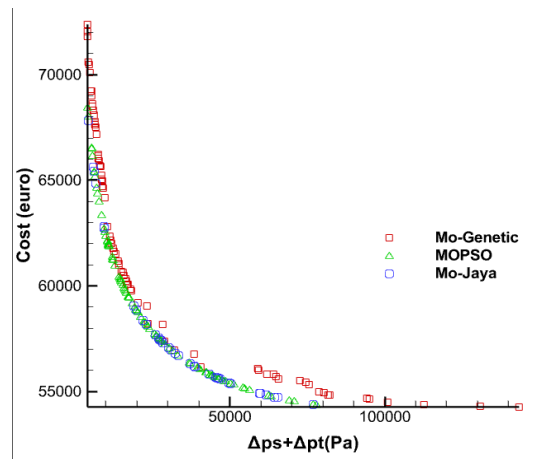


Figure 6. Comparison chart of three algorithms in terms of cost-pressure drop for case study 1.

Table 7 shows the results of each algorithm in overall heat transfer coefficient 710 (W/m².k) and total pressure drop inside of the tube and shell.

Table 7. Comparison between three optimization algorithms and reported results in table 6.

| | Present results | MO-GENETIC | MOPSO | MO-Jaya |
|------------------------------|-----------------|------------|-----------|-----------|
| UO=710 (W/m ² .K) | 62276 (€) | 61164 (€) | 60852 (€) | 60725 (€) |
| Δptotal=38549(pa) | 62276 (€) | 56788 (€) | 56290 (€) | 56145 (€) |

Based on the results, on average the Genetic algorithm improved by 9.66% compared to the present results, while the Particle Swarm algorithm improved by 10.63% compared to the present results and the Jaya algorithm improved by 10.9 compared to the genetic algorithm.

The optimization results for the second case study can also be seen in Figures 7 and 8.

Finally, due to the good performance of Jaya algorithm compared to the other two algorithms, this algorithm is applied to investigate and optimize the Ag, TiO₂ and Al₂O₃ nanofluids of various concentrations. Variation of the PEC factor for different Reynolds (for case 1) is demonstrated for various vol. concentration of Ag, TiO₂ and Al₂O₃ nanofluids in Figure 9-11.

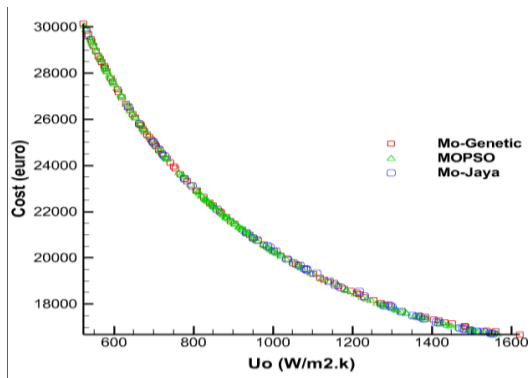


Figure 7. Comparison chart of three algorithms in terms of cost-overall heat transfer coefficient for case study 2.

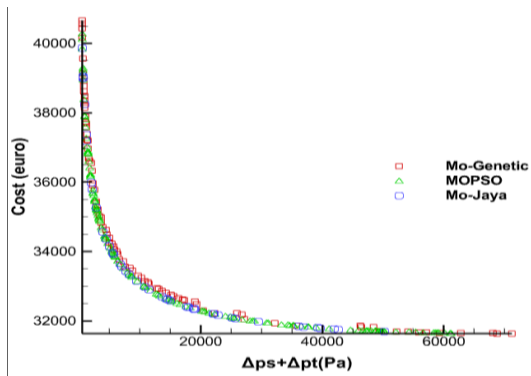


Figure 8. Comparison chart of three algorithms in terms of cost-pressure drop for case study 2.

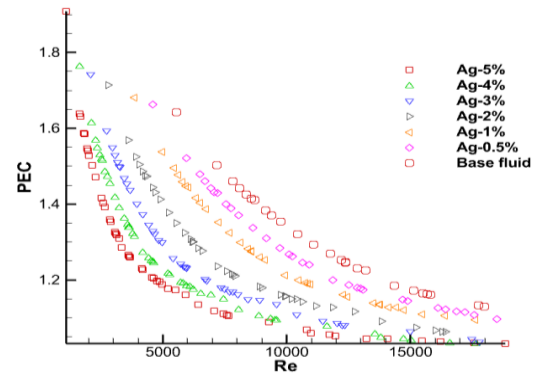


Figure 9. Comparison the results of multi objective optimization for silver (Ag) nanofluid in 0.5%-5% volume concentration based on PEC factor for case 1.

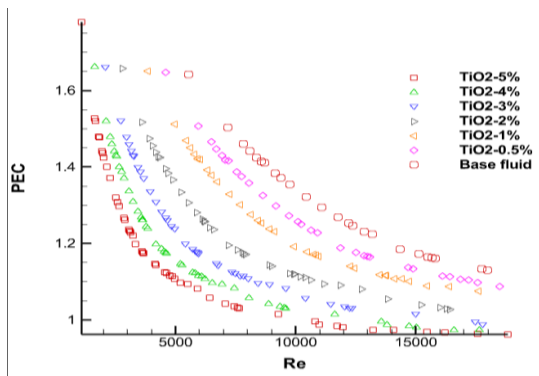


Figure 10. Comparison the results of multi objective optimization for titanium dioxide (TiO₂) nanofluid in 0.5%-5% volume concentration based on PEC factor for case 1.

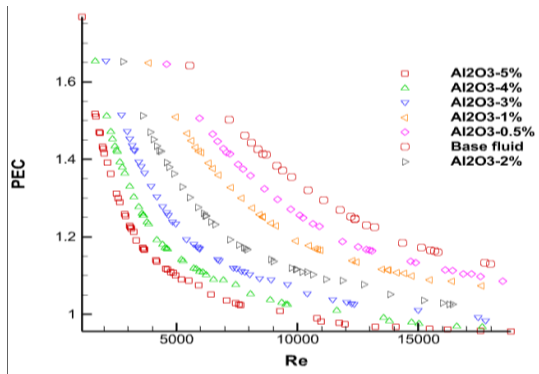


Figure 11. Comparison the results of multi objective optimization for aluminum oxide(Al₂O₃) nanofluid in 0.5%-5% volume concentration based on PEC factor for case 1.

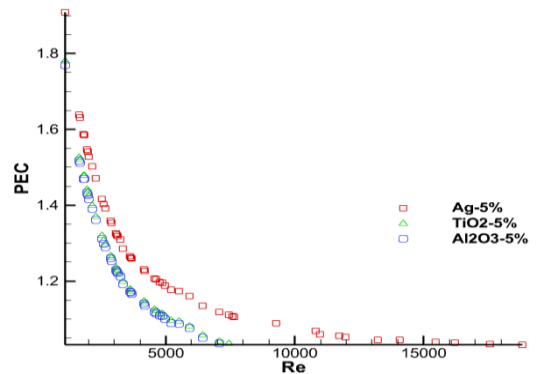


Figure 12. Comparison the results of multi objective optimization for Ag, TiO₂ and Al₂O₃ at 5% volume concentration for case 1.

In Figure 12, Variation of PEC for 5 vol. concentration of all considered nanofluids are shown.

Nanofluids as the new generation of coolants are proved to increase both heat transfer and the flow pressure drop. As much as the first effect is desirable to improve the heat exchanger efficiency, the second effect is undesirable. In this regard the trend of PEC factor is very effective in optimal thermal and hydraulic management of the heat exchanger.

By optimizing and then analyzing the results of heat exchanger according to the figures 7- 9, It is found that by increasing the nanofluid volume concentration in the constant Reynolds number, the PEC factor decreases, which means that the pressure drop decreases with increasing nanofluid volume concentration. Based on the results, the change in the Reynolds numbers at high Reynolds (for case 1 above 30000 and for case 2 above 15000) has no effect on the PEC factor, and at low Reynolds numbers the change in the Reynolds has significant effect on the PEC factor. Also, when the flow pressure drop is decision parameter, we can use the optimal point with PEC greater than one and when the flow pressure drop is not decision parameter, we can use the optimal point with PEC less than one. According to the figure 10 Silver nanofluid has more optimal points above PEC=1 and greater PEC value Comparison of to the titanium dioxide and aluminum oxide. Also according to figure 10, 5 vol% of silver nanofluid with Reynolds number 5000 for case 1 provides 5% higher PEC in comparison with pure water. While TiO2 and Al2O3 reduces PECs in comparison with pure water by about 19% and 21% respectively. The values of PEC factor for case 1 at various volume concentration and Reynolds number 5000 are demonstrated in Table 8.

Table 8. Increase/decrease percent of PEC factor for nanofluids at Reynolds number 5000 in comparison with pure water.

| Nanofluid | Ag | Tio ₂ | Al ₂ O ₃ |
|-----------|------|------------------|--------------------------------|
| 5% vol | +5% | -19% | -21% |
| 4% vol | +8% | -11% | -13% |
| 3% vol | +18% | +1.9% | +15% |
| 2% vol | +30% | +15% | +36% |
| 1% vol | +48% | +37% | +49% |
| 0.5% vol | +63% | +56% | +50% |

The same results for case 2 are also shown in Figures 13-16.

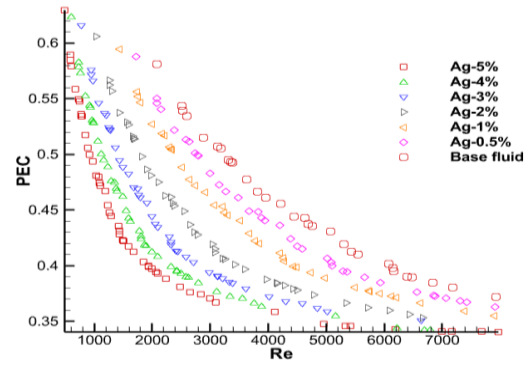


Figure 13. Comparison the results of multi objective optimization for silver (Ag) nanofluid in 0.5%-5% volume concentration based on PEC factor for case 2.

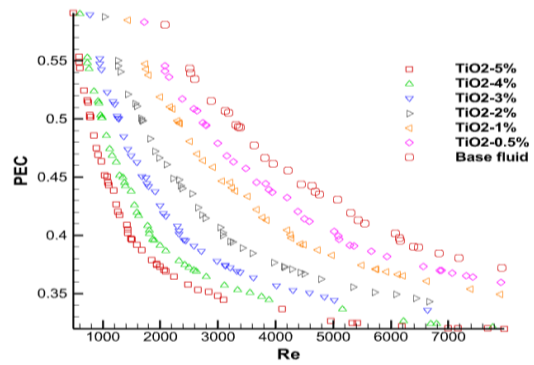


Figure 14. Comparison the results of multi objective optimization for titanium dioxide (TiO₂) nanofluid in 0.5%-5% volume concentration based on PEC factor for case 2.

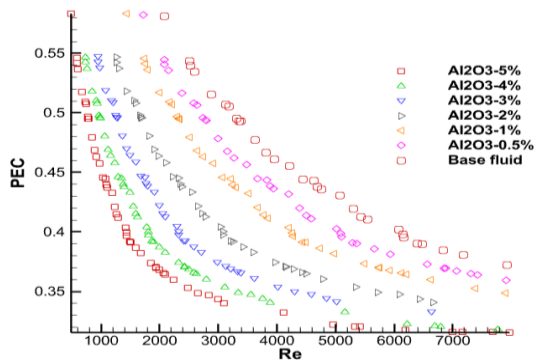


Figure 15. Comparison the results of multi objective optimization for aluminum oxide(Al₂O₃) nanofluid in 0.5%-5% volume concentration based on PEC factor for case 2.

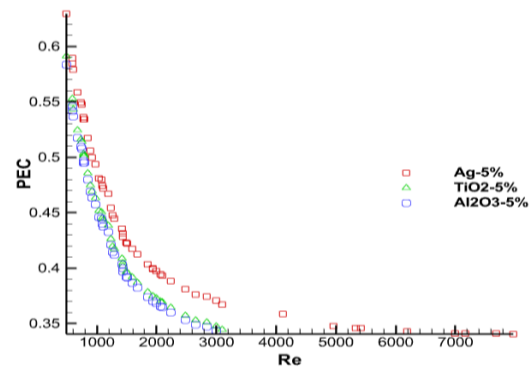


Figure 16. Comparison the results of multi objective optimization for Ag, TiO₂ and Al₂O₃ at 5% volume concentration for case 2.

According to the figures 13-16 for second case study, the PEC is less than one ($PEC < 1$). Actually, in the second case study, nanofluids increase pressure drop more than heat transfer which is as a result of lower temperature difference and less increase in heat transfer. Comparison of the increase in pressure drop with the first case study.

Conclusion

Economic issues have been an integral part of the industry. Economic constraints have always prevented many industrial activities. On the other hand, the initial costs, including the cost of construction and the necessary accessories such as pumps and so on, and operational costs including maintenance costs, fuel costs and so on, are the most important and influential parameters in industries for the selection and use of heat exchangers. In this study, a shell and tube heat exchanger was optimized by three optimization algorithms to compare and achieve better results in the multi-objective form. In any case the cost was one of the functions. In the presented charts, all points were optimal points, so according to the constraints some special points should have been chosen. These limitations include cost, length of heat exchanger, and shell diameter and so on. Also, the range of cost changes is not significant according to changes in pressure drop or heat transfer coefficient. In most of the points, there is not much difference between the three optimization algorithms, but in the application points, based on the results of the algorithm performance, the Genetic algorithm, the Particle Swarm algorithm and the Jaya algorithm has improved the present results by 9.66%, 10.63% and 10.9 % respectively. Also in terms of optimization time, Jaya optimization algorithm had relatively less time than the other two algorithms, which in fact, reduces computational costs in complex computations; that's a pretty big advantage on complex issues.

Finally, due to the good results of Jaya optimization algorithm compared to the other two algorithms, it has been employed to optimize the nanofluids in designing the heat exchanger based on PEC factor. The PEC coefficient is an effective criterion for simultaneous assessment of heat transfer and pressure drop. Actually, for the PEC factors more than one the increase in heat transfer coefficient by nanofluid is more than the corresponding pressure drop enhancement. By optimizing and analyzing the results, it was found that by increasing the nanofluid volume concentration in the constant

Reynolds number, the PEC factor decreases, which means that the pressure drop increases with increasing nanofluid volume concentration and the increase in pressure drop is greater than the increase in heat transfer coefficient. Based on the results, the change in the Reynolds numbers at low numbers has a greater effect on the PEC factor, and at high Reynolds numbers (for case 1 above 30000 and for case 2 above 15000) the change in the nanofluid volume concentration has no effect on the PEC factor. Also, when the flow pressure drop is a decision parameter, the optimal point with PEC greater than one can be chosen and when the flow pressure drop is not a decision parameter, the optimal point with PEC less than one is chosen. In fact, the nanofluid was optimized in heat exchanger and based on the results we should choose volume concentration and nanofluid based on conditions and geometry which means simultaneous optimization of nanofluid and heat exchanger according to conditions and limitations. Also it was observed that silver nanofluid has more optimal points above $PEC=1$ and greater PEC value. Comparison of to the titanium dioxide and aluminium oxide. And finally at a constant volume concentration of 5% and Reynolds number 5000, the obtained PEC of case 1 in comparison with pure water, was 5% higher, 19% lower and 21% lower for Ag, TiO_2 and Al_2O_3 nanofluids respectively.

Nomenclature

| | |
|-------------|--|
| $A_{o,cr}$ | flow area at or near the shell centerline for one cross flow section (m^2) |
| $A_{o,sb}$ | shell-to-baffle leakage flow area (m^2) |
| C_{in} | total investment cost (€) |
| C_o | annual operating cost (€/year) |
| C_{op} | total operating cost (€) |
| C_p | specific heat at constant pressure (J/kg. K) |
| C_{total} | total cost (€) |
| d_h | Hydraulic diameter (m) |
| d_i | tube side inside diameter (m) |
| d_o | tube side outside diameter (m) |
| D_{otl} | tube bundle outer diameter (m) |
| d_s | shell diameter (m) |
| F | correction factor for the number of tube passes (-) |
| h_i | tube side heat transfer coefficient ($W/m^2. K$) |
| h_o | Shell side heat transfer coefficient ($W/m^2. K$) |
| λ | annual discount rate (%) |
| J | correction factor for the shell side heat transfer |

| | |
|-----------------|---|
| k | thermal conductivity (W/m. K) |
| k_{el} | price of electrical energy (\$/kW h) |
| L | tube length (m) |
| L_{bc} | central baffles spacing (m) |
| \dot{m} | mass flow rate (kg/s) |
| N_b | number of baffles (-) |
| n_p | number of tube passes (-) |
| N_s | number of shells connected in series |
| N_t | number of tubes (-) |
| n_y | equipment life (year) |
| P | pumping power (W) |
| PEC | performance factor of nanofluids |
| Pr | Prandtl number (-) |
| P_t | tube pitch (m) |
| Q | heat transfer rate (W) |
| Re | Reynolds number (-) |
| $R_{i,f}$ | fouling resistance shell side ($m^2 \cdot K/W$) |
| $R_{o,f}$ | fouling resistance shell side ($m^2 \cdot K/W$) |
| R_b | pass correction factor |
| R_l | leakage correction factor |
| R_s | correction factor entrance and exit section |
| S | heat transfer surface area (m^2) |
| T | temperature($^{\circ}C$) |
| U | overall heat transfer coefficient ($W/m^2 \cdot K$) |
| v | velocity(m/s) |
| X_i | transverse(perpendicular to the flow) tube pitch |
| Greek symbols | |
| τ | hours of operation per year (h/year) |
| Δp | pressure drop (Pa) |
| μ | dynamic viscosity (Pa. s) |
| ρ | density (kg/m^3) |
| η | pump efficiency (-) |
| ΔT_{lm} | log-mean temperature difference |
| ϕ | volume concentration |
| Subscripts | |
| bf | base fluid |
| nf | nanofluid |
| np | nanoparticle |
| MO | Multi objective |
| i | inner |
| o | Outer |
| s | shell side |
| t | tube side |
| w | tube wall |

References

- [1] Aly, W. I. A., 2014. Numerical study on turbulent heat transfer and pressure drop of nanofluid in coiled tube-in-tube heat exchangers. *Energy Conversion and Management*, Elsevier Ltd, 79, pp. 304–316. doi: 10.1016/j.enconman.2013.12.031.
- [2] Rao, R. V., Rai, D. P. and Balic, J., 2017. A multi-objective algorithm for optimization of modern machining processes. *Engineering Applications of Artificial Intelligence*. Elsevier Ltd, 61(March), pp. 103–125. doi: 10.1016/j.engappai.2017.03.001.
- [3] Arsana, I. M. and Rahardjo, M. A. H., 2020. Simulation study on efficiency of woven matrix wire and tube heat exchanger. *International Journal of Engineering Transactions C: Aspects*, 33(12), pp. 2572–2577. doi: 10.5829/ije.2020.33.12c.19.
- [4] Atapattu, S., Tellambura, C. and Jiang, H., 2014, Performance measurements. *SpringerBriefs in Computer Science*, 0(9781493904938), pp. 41–62. doi: 10.1007/978-1-4939-0494-5_4.
- [5] Balamurugan, S. and Samsoloman, D. P., 2014. *Experiment*. 00(2013), pp. 59–66.
- [6] Baniamerian, Z., Mehdipour, R. and Murshed, S. M. S., 2019. An experimental investigation of heat of vaporization of nanofluids. *Journal of Thermal Analysis and Calorimetry*, doi: 10.1007/s10973-019-08202-y.
- [7] Bock Choon Pak, Y. I. C., 2013. Hydrodynamic and Heat Transfer Study of Dispersed Fluids With Submicron Metallic Oxide. *Experimental Heat Transfer: A Journal of Thermal Energy Transport, Storage, and Conversion*, January 2013, pp. 37–41.
- [8] Borzuei, M. and Baniamerian, Z., 2020. Role of nanoparticles on critical heat flux in convective boiling of nanofluids: Nanoparticle sedimentation and Brownian motion. *International Journal of Heat and Mass Transfer*, Elsevier Ltd, 150, p. 119299. doi:10.1016/j.ijheatmasstransfer.2019.119299.
- [9] Dalkılıç, A. S. et al., 2020. Optimization of the finned double-pipe heat exchanger using nanofluids as working fluids. *Journal of Thermal Analysis and Calorimetry*, Springer International Publishing, 5(0123456789). doi: 10.1007/s10973-020-09290-x.
- [10] Ghorbani, M. and Ranjbar, S. F., 2019. Optimization of compressed heat exchanger efficiency by using genetic algorithm. *International Journal of Applied Mechanics and Engineering*, 24(2), pp. 461–472. doi: 10.2478/ijame-2019-0029.

- [11] GUTHRIE KM., 1969. Capital Cost Estimating. Chemical Engineer, doi: 10.1021/ie50502a032.
- [12] Hajabdollahi, Z., Hajabdollahi, H. and Kim, K. C., 2020. Heat transfer enhancement and optimization of a tube fitted with twisted tape in a fin-and-tube heat exchanger. *Journal of Thermal Analysis and Calorimetry*, Springer International Publishing, 140(3), pp. 1015–1027. doi: 10.1007/s10973-019-08668-w.
- [13] Hanson, F. V., 1989. Heat exchangers selection, design and construction. *Fuel Processing Technology*, pp. 87–88. doi: 10.1016/0378-3820(89)90046-5.
- [14] Hoghoj, L. C. et al., 2020. Topology optimization of two fluid heat exchangers. *International Journal of Heat and Mass Transfer*, 163(July). doi: 10.1016/j.ijheatmasstransfer.2020.120543.
- [15] Hojjati, A. et al., 2018. Application and comparison of NSGA-II and MOPSO in multi-objective optimization of water resources systems. *Journal of Hydrology and Hydromechanics*, 66(3), pp. 323–329. doi: 10.2478/johh-2018-0006.
- [16] Jeklin, A., 2016. 濟無 No Title, *vol, 1*, pp.1-23.
- [17] John, A. K. and Krishnakumar, K., 2017. Performing multiobjective optimization on perforated plate matrix heat exchanger surfaces using genetic algorithm. *International Journal for Simulation and Multidisciplinary Design Optimization*, 8, pp. 0–7. doi: 10.1051/smdo/2016011.
- [18] Khanmohammadi, Shoaib *et al.*, 2020. Triple-objective optimization of a double-tube heat exchanger with elliptic cross section in the presence TiO₂ nanofluid. *Journal of Thermal Analysis and Calorimetry*, Springer International Publishing, 140(1), pp. 477–488. doi: 10.1007/s10973-019-08744-1.
- [19] Khoshvaght-Aliabadi, M., 2014. Influence of different design parameters and Al₂O₃-water nanofluid flow on heat transfer and flow characteristics of sinusoidal-corrugated channels. *Energy Conversion and Management*, Elsevier Ltd, 88, pp. 96–105. doi: 10.1016/j.enconman.2014.08.042.
- [20] Maïga, S. E. B. *et al.*, 2006. Heat transfer enhancement in turbulent tube flow using Al₂O₃ nanoparticle suspension. *International Journal of Numerical Methods for Heat and Fluid Flow*, 16(3), pp. 275–292. doi: 10.1108/09615530610649717.
- [21] Memari, A., Rahim, A. R. A. and Ahmad, R. B., 2015. An integrated production-distribution planning in green supply chain: A multi-objective evolutionary approach. *Procedia CIRP*, Elsevier B.V., 26(September 2014), pp. 700–705. doi:10.1016/j.procir.2015.03.006.
- [22] McDonald, A. G. and Magande, H. L., 2012. Fundamentals of Heat Exchanger Design. *Introduction to Thermo-Fluids Systems Design*, pp. 127–211. doi: 10.1002/9781118403198.ch4.
- [23] Miansari, M. et al., 2020. Energy and exergy analysis and optimization of helically grooved shell and tube heat exchangers by using Taguchi experimental design. *Journal of Thermal Analysis and Calorimetry*, Springer International Publishing, 139(5), pp. 3151–3164. doi: 10.1007/s10973-019-08653-3.
- [24] Najafi, H. and Najafi, B., 2010. Multi-objective optimization of a plate and frame heat exchanger via genetic algorithm. *Heat and Mass Transfer/Waerme- und Stoffuebertragung*, 46(6), pp. 639–647. doi: 10.1007/s00231-010-0612-8.
- [25] Rao, R. V., Rai, D. P. and Balic, J., 2017. A multi-objective algorithm for optimization of modern machining processes. *Engineering Applications of Artificial Intelligence*, Elsevier Ltd, 61(March), pp. 103–125. doi: 10.1016/j.engappai.2017.03.001.
- [26] Rohsenow Editor, W. M. et al., 1998. HANDBOOK OF HEAT TRANSFER MCGRAW-HILL Chapter 1. Basic Concepts of Heat Transfer 1.1 The Equation of Motion (Momentum Equation) / Chapter 2. Thermophysical Properties 2.1', *Handbook of Heat Transfer*.
- [27] Sadeghzadeh, H., Aliehyaei, M. and Rosen, M. A., 2015. Optimization of a finned shell and tube heat exchanger using a multi-objective optimization genetic algorithm. *Sustainability (Switzerland)*, 7(9), pp. 11679–11695. doi: 10.3390/su70911679.
- [28] Sadeghzadeh, H., Ehyaei, M. A. and Rosen, M. A., 2015. Techno-economic optimization of a shell and tube heat exchanger by genetic and particle swarm algorithms. *Energy Conversion and Management*. Elsevier Ltd, 93, pp. 84–91. doi: 10.1016/j.enconman.2015.01.007.
- [29] Shoheib, M. M., Hamzehei, M. and Shahrooi, S., 2019. Investigating tubes material selection on thermal stress in shell side inlet zone of a vertical shell and tube heat exchanger. *Journal of Heat and Mass Transfer Research*, 6(2), pp. 21–30. doi: 10.22075/jhmtr.2018.14041.1203.
- [30] Sieder, E. N. and Tate, G. E., 1936. Heat Transfer and Pressure Drop of Liquids in Tubes. *Industrial and Engineering Chemistry*, 28(12), pp. 1429–1435. doi: 10.1021/ie50324a027.

- [31] Taal, M. et al., 2003. Cost estimation and energy price forecasts for economic evaluation of retrofit projects. *Applied Thermal Engineering*, 23(14), pp. 1819–1835. doi: 10.1016/S1359-4311(03)00136-4.
- [32] Taghilou, M., Ghadimi, B. and Seyyedvalilu, M. H., 2014. Optimization of Double Pipe Fin-pin Heat Exchanger using Entropy Generation Minimization. *International Journal of Engineering*, 27(9 (C)), pp. 1431–1438. doi: 10.5829/idosi.ije.2014.27.09c.13.
- [33] Turgut, O. E., 2017. Multi-objective thermal design optimization of plate frame heat exchangers through Global Best Algorithm. Bitlis Eren University, *Journal of Science and Technology*, 7(1), pp. 33–33. doi: 10.17678/beuscitech.322141.
- [34] Uddin, M. J., Rahman, M. M. and Alam, S., 2016. Fundamentals of Nanofluids: Evolution, Applications and New Theory. *International Journal of Biomathematics and Systems Biology*, 2(1), pp. 1–31.
- [35] Valipour, M. S., Biglari, M. and Assareh, E., 2016. Thermal-Economic Optimization of Shell and Tube Heat Exchanger by using a new Multi-Objective optimization method. *Journal of Heat and Mass Transfer Research (JHMTR)*, 3(1), pp. 67–76.
- [36] Zhao, L., Huo, Z. and Yin, H., 2013. Heat exchanger network optimization considering pressure drop constraints based on minimum operating cost. *International Journal of Online Engineering*, 9 (SPECIALISSUE.6), pp. 33–37. doi: 10.3991/ijoe.v9iS6.2798.